ELSEVIER

Earth and Planetary Science Letters 157 (1998) 9–22

EPSL

Self-consistent generation of tectonic plates in three-dimensional mantle convection

Paul J. Tackley *

Department of Earth and Space Sciences, University of California, Los Angeles, 405 Hilgard Avenue, Los Angeles, CA 90095-1567, USA

Received 25 September 1997; revised version received 30 January 1998; accepted 5 February 1998

Abstract

Despite the fundamental importance of plates in the Earth's mantle convection, plates have not generally been included in numerical convection models or analog laboratory experiments, mainly because the physical properties which lead to plate tectonic behavior are not well understood. Strongly temperature-dependent viscosity results in an immobile rigid lid, so that plates, where included at all in 3-D models, have always been imposed by hand. An important challenge is thus to develop a physically reasonable material description which allows plates to develop self-consistently; this paper focuses on the role of ductile shear localization. In two-dimensional geometry, it is well-established that strain-rate softening, non-Newtonian rheologies (e.g. power-law, visco-plastic) cause weak zones and strain-rate localization above up- and down-wellings, resulting in a rudimentary approximation of plates. Three-dimensional geometry, however, is fundamentally different due to the presence of transform plate boundaries with associated toroidal motion. Since power-law and visco-plastic rheologies do not have the property of producing shear localization, it is not surprising that they do not produce good plate-like behavior in three-dimensional calculations. Here, it is argued that a strain-rate-weakening rheology, previously shown to produce plate-like behavior in a two-dimensional sheet representing the lithosphere, is a reasonable generic description of various weakening processes observed in nature. One- and two-dimensional models are used to show how this leads to shear localization and the formation of 'faults'. This rheology is then applied to the high-viscosity lithosphere of 3-D mantle convection calculations, and the velocity-pressure/viscosity solution for the entire 3-D domain (lid and underlying mantle) is solved self-consistently. It is found that the lithosphere divides into a number of very high-viscosity plates, separated by narrow, sharply defined weak zones with a viscosity many orders of magnitude less than the plate interiors. Broad weak zones with dominant convergent/divergent motion above up- and down-wellings are interconnected by a network of narrow weak zones with dominant strike-slip motion. Passive spreading centers are formed in internally heated cases. While the resulting plates are not fully realistic, these results show that self-consistent plate generation is a realizable goal in three-dimensional mantle convection, and provide a promising avenue for future research.

Keywords: plate tectonics; plates; mantle; convection; models

* Tel.: +1 (310) 206-9180; Fax: +1 (310) 825-2779; E-mail: ptackley@ess.ucla.edu

0012-821X/98/$19.00
PII S0012-821X(98)00029-6

1. Introduction

Plate tectonics is arguably the most important manifestation of mantle convection. However, it is a long-standing problem that mantle convection experiments, either computational or laboratory, do not naturally develop plate tectonics. Strongly temperature-dependent viscosity is clearly an important ingredient, but this leads to an immobile, rigid lid, essentially a single plate covering the entire planet [1,2]. Thus, it has been necessary to impose plates by hand, either as a velocity boundary condition (e.g. [3]), or by specifying the locations of weak zones (WZs) or faults (e.g. [4,5]). A long-standing and fundamental challenge in geodynamics is to identify a physically reasonable material description which allows plates to form self-consistently, rather than being imposed by the modeler.

'Real' plate margins are thought to involve faults in the crust and upper lithosphere where brittle and elastic modes of deformation are important, with ductile shear zones below this depth [6–8]. It is not clear what the relative importance of brittle faults versus ductile shear localization is in producing plate margins, since the brittle and ductile layers are of comparable strength, and the crust is often decoupled from the mantle lithosphere by the weak lower crustal layer. Perhaps brittle failure occurs first, guiding the locations for ductile shear localization [7]. However, in some cases, ductile shear localization is observed to precede brittle failure [9]. In any case, the mantle convection community has focused on the role of ductile strain-rate localization mechanisms, an approach which is continued in the present study.

In two-dimensional geometry (2-D), it is well-established that strain-rate softening, non-Newtonian rheologies cause weak zones (WZs) and strain-rate localization above up- and down-wellings [10,11], resulting in a rudimentary approximation of plates [12,13]. This is easy to understand since in 2-D, there are only convergent and divergent margins, which have concentrated buoyancy/stress sources below them to 'break' the rigid lid and focus deformation. Three-dimensional geometry (3-D) is fundamentally more challenging due to the transform (strike-slip) boundaries, associated with toroidal motion, which makes up almost half of the total plate velocity field [14]. There are no concentrated local buoyancy forces available to drive and localize transform boundaries; indeed, buoyancy in the mantle cannot directly drive toroidal motion at all if the viscosity is purely depth-dependent [15,16]. Thus, it is not surprising that the rheologies that produce reasonable 'plates' in 2-D do not work well in 3-D [17–19].

Real upper mantle shear zones are commonly observed in large massifs in orogenic belts [20,21], a particularly notable, 170-km-long example of which is observed in west Greenland [22]. When formed at moderate temperatures (i.e., less than about 950°C) and high stresses, these shear zones are narrow (from cm to km width) and contain mylonites, a type of rock characterized by strong grain-size reduction and (commonly) hydration [21].

What physical mechanism(s) could be responsible for such shear zones? Shear localization requires 'self-lubrication' or strain weakening (i.e., the stress required to maintain a given strain rate decreases with increasing strain), for which several mechanisms have been proposed: (1) grain-size reduction due to dynamic recrystallization, which can lead to a transition from grain-size insensitive dislocation creep to grain-size sensitive diffusion creep, with a potential viscosity reduction of many orders of magnitude. Field observations [9,20,21,23], laboratory experiments [24,25], and 1-D numerical models [26] strongly support this mechanism; (2) production of voids (pores and microcracks) followed by volatile ingestion, again indicated by field observations [27,28]; (3) the feedback between viscous dissipation and temperature-dependent viscosity [29,30], for which some field evidence exists [31]; and (4) damage theory (e.g. [32–34]), which involves the weakening of material by 'damage' (production of microcracks, voids, etc.), although this is more oriented towards the seismogenic zone. In the remainder of this paper, however, the term 'damage' will be used to refer to any of the above weakening mechanisms (i.e. grain-size reduction, voids, microcracks, volatile infiltration, temperature increase).

These mechanisms all cause strain weakening. However, the 'damage' also heals with time, due to annealing or diffusional processes. Using suitable parameterizations of these mechanisms, one can derive a 'steady-state', in which production of damage (described by a damage vs. strain relation-

ship) is balanced by healing (described by a damage vs. time relationship) to give a damage vs. strain-rate relationship, and hence (through a viscosity vs. damage relationship) a stress vs. strain-rate relationship. Examples for the viscous dissipation and void–volatile mechanisms are derived in [27]. In all cases, the stress increases with strain-rate to some critical point, after which further strain rate leads to weakening, i.e. stress reduction. Such a strain-rate-weakening (SRW) rheology thus appears to be a robust, generic description of the physical processes which can lead to shear localization. Whether such a 'steady-state' is actually attained in nature depends on the time-scales for damage production and healing relative to the time-scale on which driving force or deformation is applied. For the purposes of obtaining a basic, first-order understanding of the underlying physics, a 'steady-state' SRW rheology is adopted in this paper. The details of the time-evolution of damage and shear localization must certainly be addressed in future.

Particular examples of this SRW rheology have been successfully applied to the problem of plate generation in a two-dimensional lithospheric sheet by Bercovici [19,35], with deformation of the sheet driven by specified sinks and sources. The models showed that SRW rheology, in the form of a general 'stick–slip, rheology [19,35], viscous-dissipation feedback [36], or void-volatile self-lubrication [27], is extremely effective in producing self-localization of shear and very narrow shear bands which give a good approximation of transform faults.

In this paper, SRW rheology is applied to the high-viscosity lithosphere of 3-D mantle convection calculations, with driving stresses derived from thermal buoyancy of up- and down-wellings. These solutions are preceded by simple one- and two-dimensional analyses to gain an understanding of how the self-localization works.

2. Strain-rate-weakening rheology

As argued above, a strain-rate-weakening (SRW) effective rheology is a consequence of combining strain weakening by some type of 'damage', with time-dependent healing of the damage. The form of SRW rheology adopted here arises under the following generic conditions: (1) the rate of damage production is proportional to the product of stress and strain rate, i.e. the rate at which work is done on the system; (2) the rate of healing of damage is proportional to the amount of damage (i.e. an exponential decay), although this is more complicated for grain-size reduction [26]; and (3) viscosity decreases linearly with increasing damage. A 'steady-state' stress vs. strain-rate relationship can be derived by equating damage-production rate to healing rate, then using the viscosity vs. damage relationship to obtain viscosity as a function of strain rate:

$$\sigma_{ij} = 2\frac{\sigma_{\text{yield}}^2 \eta}{\sigma_{\text{yield}}^2 + \eta^2 \dot{e}^2}\dot{e}_{ij} \equiv 2\eta_{\text{eff}}\dot{e}_{ij} \tag{1}$$

where σ = stress, η = viscosity for 'undamaged' material, σ_{yield} = yield stress (the maximum possible stress), η_{eff} = 'effective' viscosity, and the scalar strain rate $\dot{e}$ is similar to the second invariant of the deviatoric strain-rate tensor:

$$\dot{e} = \sqrt{\dot{e}_{ij}\dot{e}_{ij}} \tag{2}$$

This is very similar to the stress vs. strain-rate relationship obtained by Bercovici for viscous-dissipation [36] or void-volatile self-lubrication [27], but differs by being parameterized in terms of yield stress and 'undamaged' viscosity. Asymptotically, for small the material behaves like a Newtonian fluid with the 'undamaged' viscosity, whereas for large $\dot{e}$, stress is inversely proportional to strain rate.

3. One-dimensional model

We first consider a 1-D model, in which a domain of length l is sheared with velocity V. There is only one stress component (the shear stress), and the momentum equation reduces to:

$$\sigma = \text{constant} \tag{3}$$

where σ = shear stress, with the boundary condition

$$\int_0^l \dot{e} = V \tag{4}$$

where $\dot{e}$ = shear strain rate, defined here as the velocity gradient, twice the conventional definition. For the purposes of analysis, a simplified SRW rheology

is assumed, with the following form:

$$\sigma = \begin{cases} \eta\dot{e} & \dot{e} \le \sigma_{\text{yield}}/\eta \\ \sigma_{\text{yield}}^2/\eta\dot{e} & \dot{e} > \sigma_{\text{yield}}/\eta \end{cases} \quad (5)$$

This has the same asymptotic slopes as the full rheology (Eq. (1)). Viscosity η and yield stress σ_{yield} are both taken to be unity for this 1-D analysis. The maximum possible stress is thus 1, with two possible strain-rate values for a particular value of stress. These two values can be called the 'plate' and 'weak' branches. Thus:

$$\sigma = \text{constant} = \dot{e}_{\text{plate}} = 1/\dot{e}_{\text{weak}} \quad (6)$$

In order to satisfy the boundary condition for general σ and V, it is necessary for some fraction W of the domain to be on the weak branch, with the remainder on the plate branch. It is straightforward from Eq. (6) and matching the velocity boundary condition (i.e. $W\dot{e}_{\text{weak}} + (1-W)\dot{e}_{\text{plate}} = V$) to derive relationships for W as function of V and σ, or σ as a function of V and W:

$$W = \frac{V-\sigma}{(1/(\sigma-\sigma)}, \quad \sigma = \frac{V \pm\sqrt{V^2 - 4(1-W)W}}{2(1-W)} \quad (7)$$

Thus, for each value of imposed velocity V, there is a continuum of solutions with different σ and W. These are illustrated in Fig. 1. For $V < 1$ there are two possible solutions for each W, one with high stress (a modulation of uniform shear) and one with low stress (in which most of the shear occurs across the WZ), but for $V > 1$ there is only one solution for each W. Which solution will the system choose? A reasonable assumption is that is will choose the solution which minimizes dissipation, which in this case is equivalent to minimization of stress (because stress is constant). The resulting solution is:

$$\sigma = 0, \quad W = 0, \quad \dot{e}_{\text{weak}} = \infty, \quad \dot{e}_{\text{plate}} = 0 \quad (8)$$

This describes a fault with zero strength: away from the fault the medium is rigid, with all shear taken up in the infinitely narrow fault region. Would the system really choose this solution? A couple of physical arguments can be made to support this: (1) the negative stress/strain-rate gradient in the 'weak' branch implies a negative 'incremental viscosity' [19]. Since viscosity can be regarded as a diffusion coefficient for strain rate, and normally (for positive values) spreads out the strain for a focused driving stress, this will tend focus the strain rate; and (2) during the process of formation of these 'faults', which corresponds numerically to successive iterations, or physically, to time evolution of a strain-weakening mechanism, some regions will have higher strain-rates than others. These higher strain-rate regions become weaker, while lower strain-rate regions become stronger, further accentuating the differences in strain rate, and eventually leading to a narrow weak 'fault' amidst strong surroundings.

The solution does not specify where the WZ forms in the domain: it could be anywhere. This inherent multi-valuedness of the solution is a point that is returned to later.

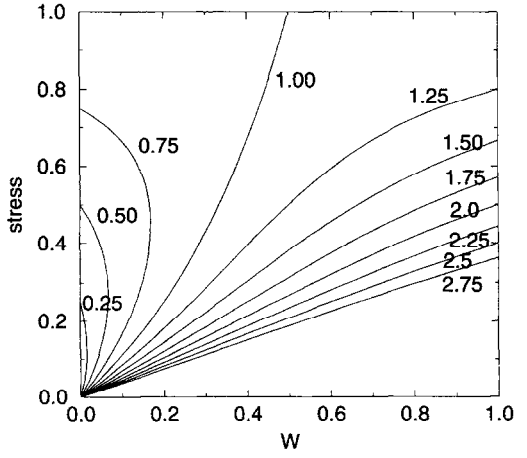

Fig. 1. Relationship between stress and weak zone width, W, for one-dimensional shear with various values of imposed velocity, V (marked on curves).

3.1. Other rheologies

How does this process depend on the details of rheology, in particular, the slope of stress/strain-rate relationship past the yield point for a 'steady-state' description? The above analysis will lead to the same 'weak fault' solution for any negative stress/strain-rate slope. For a positive slope, there is only one possible strain rate for each stress, leading to a unique solution: constant velocity gradient, viscosity and strain rate. How about a pure visco-plastic rheology, where the stress saturates past the yield point? Local strain rate can take on any value past the critical one, leading to an infinite number of possible

solutions. These range from a constant strain rate (velocity gradient) across the domain, to strain localization in one or more narrow 'faults' with the rest of the domain having a strain rate (velocity gradient) which is at the critical value. So, shear localization is a possible solution, but: (1) in the visco-plastic case, localization is a possible solution, but not the preferred solution, whereas the strain-rate-weakening rheology naturally results in localization; and (2) the stress across the domain is still high (i.e. the yield stress) in the visco-plastic case, but goes to zero in the strain-rate-weakening case.

3.2. Underlying mantle

A simple approximation of the effect of an underlying mantle layer can be obtained by 'welding' a weak mantle asthenospheric layer to the 1-D lithosphere, such that stress for strain rates past the critical value is now given by:

$$\sigma = \dot{e}^{-1} + \eta_m \dot{e} \tag{9}$$

where η_m is the viscosity of the mantle, which is much less than 1. Increasing the strain rate then only decreases stress up to a point, given by

$$\dot{e}_{min} = \left(\frac{1}{\eta_m}\right)^{1/2} \tag{10}$$

beyond which stress increases. If the system acts to minimize dissipation and thus stress, the strain rate in the WZ will be equal to this value, strain rate in 'plate' regions will be finite, as will stress across the domain. Thus, the asthenospheric layer limits the degree of localization that is possible in the lithospheric layer.

4. Two-dimensional model

The model is now extended to a 2-D cross-section across the lithosphere and upper asthenosphere, which are taken to be of equal thickness, nominally 100 km, and have 'undamaged' viscosities of 1 and 10^{-4} respectively, plus small random perturbations to provide a preferred location for 'fault' formation. With the cross-section in the (x, z) plane, where z is vertical, the momentum equation becomes:

$$(\eta v_{x,y})_{,x} + (\eta v_{y,z})_{,z} = 0 \tag{11}$$

with $v_x = v_z = 0$. Side boundaries have a constant v_y of 0 (left) or 1 (right) with top and bottom boundaries stress-free. The solution is obtained numerically, by iterating between the effective viscosity field (initialized at the undamaged viscosity), and the velocity solution (obtained using a direct solver).

Fig. 2 shows a comparison of results for Newtonian viscosity, and for the strain-rate-weakening (SRW) rheology with $\sigma_{yield} = 0.5$. The Newtonian case shows, as expected, uniform velocity gradient across the domain, and a stress of 1.0 in the lithosphere and 10^{-4} in the lower layer. In contrast, the lithospheric deformation in the SRW case is concentrated into one weak 'fault' visible in the viscosity field, with velocity nearly uniform on either side of the fault but discontinuous across it. In the weak lower layer, deformation is more distributed. The maximum stress value has dropped 3.5 orders of magnitude compared to the Newtonian case. Other cases indicate that the degree of localization depends on the rate of drop-off of stress with strain-rate (faster drop-off results in greater focusing), and viscosity contrast between the layers (as predicted in 1-D).

5. Three-dimensional model

The case of a strong lithosphere underlain by an isoviscous mantle is now considered. The lithosphere is taken to be a constant-thickness layer approximately 100 km thick with an undamaged viscosity of 10^4, while the underlying mantle has an undamaged viscosity of 1.0.

A major conceptual difference exists between these cases and the preceding 1- and 2-D analyses in that the system is driven by fixed sources of stress (thermal buoyancy) rather than fixed sources of strain rate (velocity boundary conditions). If the 1- and 2-D cases were driven by fixed shear stress rather than fixed velocities, solutions would diverge to infinity because stress decreases with increasing strain rate. However, in 3-D, the bulk of the mantle, which is not in the SRW regime, limits the maximum velocities that can be obtained: even if the lithosphere tended towards zero strength, flow velocities would saturate and not approach infinity.

The experimental procedure is as follows: (1) temperature fields are taken from constant-viscos-

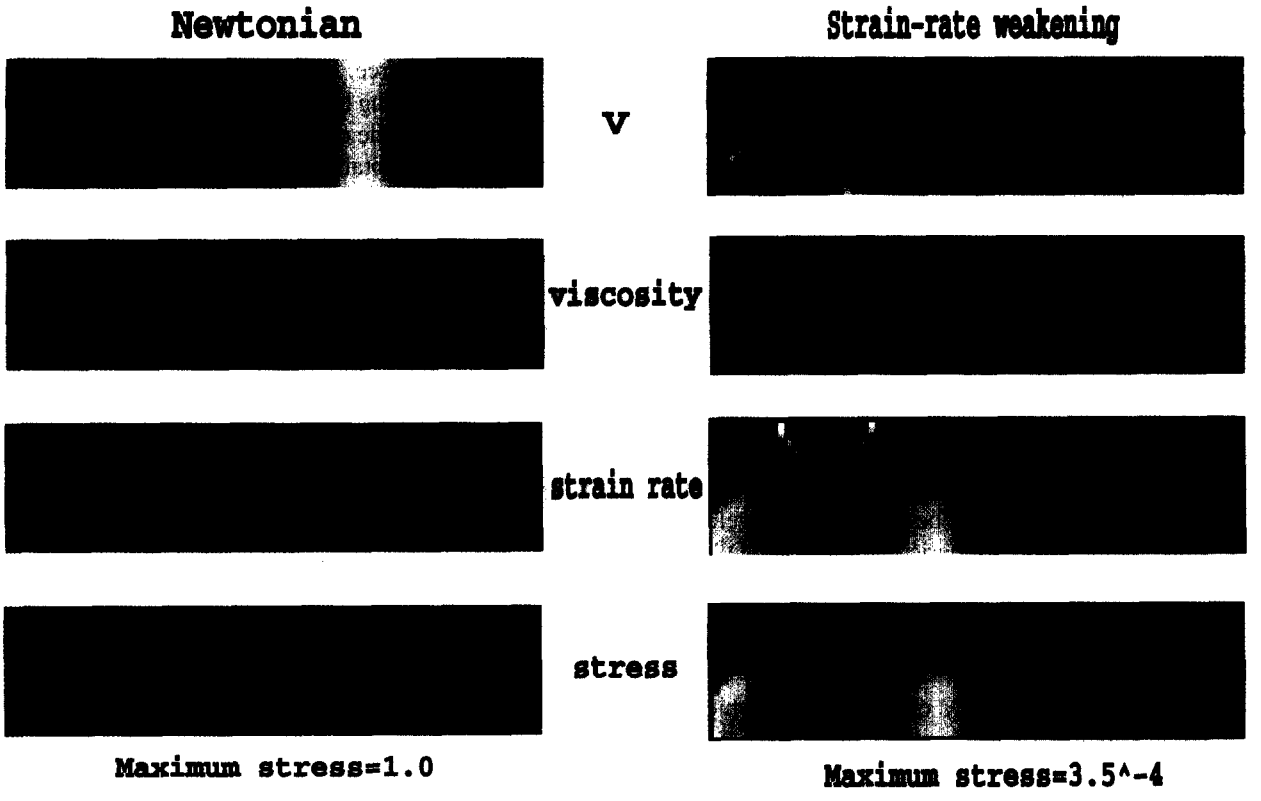

Fig. 2. Two-dimensional model of lithospheric and asthenospheric shear, with Newtonian rheology (left) and SRW rheology (right). Velocity (top), viscosity (2nd row), strain rate (3rd row) and stress (bottom). A standard blue-green-red colorbar is used, scaled to minimum and maximum values, respectively.

ity, 3-D calculations which have reached statistically steady-state; and (2) the instantaneous velocity-pressure/viscosity solutions for the same systems, but with layered, SRW rheology are calculated self-consistently for the entire domain. This involves (a) initializing the viscosity field to a value of 1.0 everywhere, then (b) iterating between the velocity-pressure solution, calculated from the usual mantle convection equations using a finite-volume multigrid technique, both fully described elsewhere [37,38], and the viscosity solution, calculated from Eq. 1. Roughly 30–60 iterations are necessary to achieve convergence. The subsequent time evolution of the system is not considered here.

Solutions are not strongly dependent on the exact value of yield stress, except that a homogeneous rigid lid is obtained if it is too high. Lower values lead to broader WZs, but the same basic pattern. Here, we choose a value just below that which would cause a rigid lid ($\sim 2(\eta\dot{e})_{\max}$ for Newtonian rheology). This is different for Case 4 because of the quite different Ra and other parameters.

Numerical resolution is generally 32 cells in the vertical direction (the lithosphere constitutes the upper layer of cells), with a proportional number in the horizontal directions. Convergence tests indicate that numerical resolution does not make very much difference provided it is high enough for strain rates to extend well into the 'weak' branch: with too low resolution the solution decays into a homogeneous rigid lid.

Table 1 lists the cases presented. Boussinesq cases have constant physical properties except viscosity, whereas compressible cases have depth-dependent expansivity, diffusivity, and density in a compressible anelastic approximation described in [38]. The quoted Rayleigh number is based on the mantle viscosity (= 1) and (in the compressible cases), surface

Table 1
The four 3-D cases

Case	Approx.	Domain	BCs	Heating	Ra	σ_{yield}
1	B	$1 \times 1.4 \times 1$	R	Basal	10^5	10^5
2	B	$8 \times 8 \times 1$	P	Basal	10^5	10^5
3	B	$2 \times 2 \times 1$	P	Internal	10^5, 10^6	10^5
4	C	$4 \times 4 \times 1$	R	Basal	10^6	10^6

B = Boussinesq, C = compressible, BCs = side boundary conditions, R = reflecting, P = periodic, Ra = Rayleigh number.

values of thermal expansivity, thermal diffusivity, and density. Both temperature-based and heating-based Ra are given for Case 3.

5.1. Small domain

The temperature field for Case 1 (Fig. 3a) contains a down-welling at one corner of the box and an up-welling at the opposite corner. The dominant features in the viscosity/velocity solution (Fig. 3b) are two high-viscosity plate-like regions surrounded by WZs. One plate is moving diagonally across the box, while the other is stationary, with a weak shear zone in-between. The formation of a localized shear zone away from any up- and down-wellings is a very encouraging feature of this solution. WZs also form above up- and down-wellings, as expected. The boundary between WZ and 'plate' is very sharp, with a large viscosity jump occurring over one grid cell. This is a characteristic of the SRW rheology, occurring because continuity of stress requires that the strain rate flip from 'plate' branch to 'weak' branch discontinuously.

Vertical vorticity and horizontal divergence are shown in Fig. 3c. Convergent and divergent regions are focused at the down- and up-welling, respectively. Vertical vorticity, an indicator of strike-slip motion, is concentrated in a line following the shear plate margin. All quantities are concentrated in the lithosphere, with secondary divergence peaks at the base of the mantle.

5.2. Wide domain

Is the solution in Case 1 simply a result of the small domain and reflecting sides? To address this concern, Case 2 has the same parameters except in a wide ($8 \times 8 \times 1$) box with periodic sides. The temperature field (Fig. 4a) has a pattern of up- and down-wellings characteristic of Boussinesq, constant-properties, basally heated convection at this Ra. Examination of the lithospheric viscosity and velocity fields (Fig. 4b) again shows a pattern of strong plates separated by narrow WZs. WZs form above the up- and down-wellings (as expected from the stress concentration there), but more importantly, also connect the up-/down-wellings together. The WZs above up- and down-wellings have a width comparable to the width of the convective feature, which is expected because the region of high stress associated with the feature has this characteristic size. These WZ are associated with strong convergence and divergence (Fig. 4b), while the interconnecting zones localize down to a size which is limited by the viscosity of the underlying medium (as shown by the 1- and 2-D analyses), and are associated with high vertical vorticity. Some of the plates have strong rotation which also shows up in the vorticity. While the plate boundaries appear to be well separated into divergent and strike-slip in this figure, they generally include both strike-slip and convergent/divergent motion.

A visco-plastic rheology is much less effective in producing plate-like behavior (Fig. 4d). WZs occur above up- and down-wellings but not in-between. Regions of high vorticity now cluster around the convergent/divergent regions, i.e. where the lid is already weakened, compatible with previous results of convection with temperature-dependent viscosity [39,40].

5.3. Internal heating (Fig. 5)

Down-wellings in internally heated convection (e.g. [41,42]) are point-like, occasionally slightly elongated. The plate pattern produced is quite different from the basally heated cases, being characterized by small, mobile microplates surrounding the down-wellings, embedded in an otherwise stagnant lid. The elongated down-welling at the lower left is perhaps the easiest to understand: here, two microplates move from passive spreading centers (i.e. spreading centers which are not above a deep-seated, focused mantle up-welling) towards the down-welling, with transform margins at each end. The configuration around cylindrical down-wellings

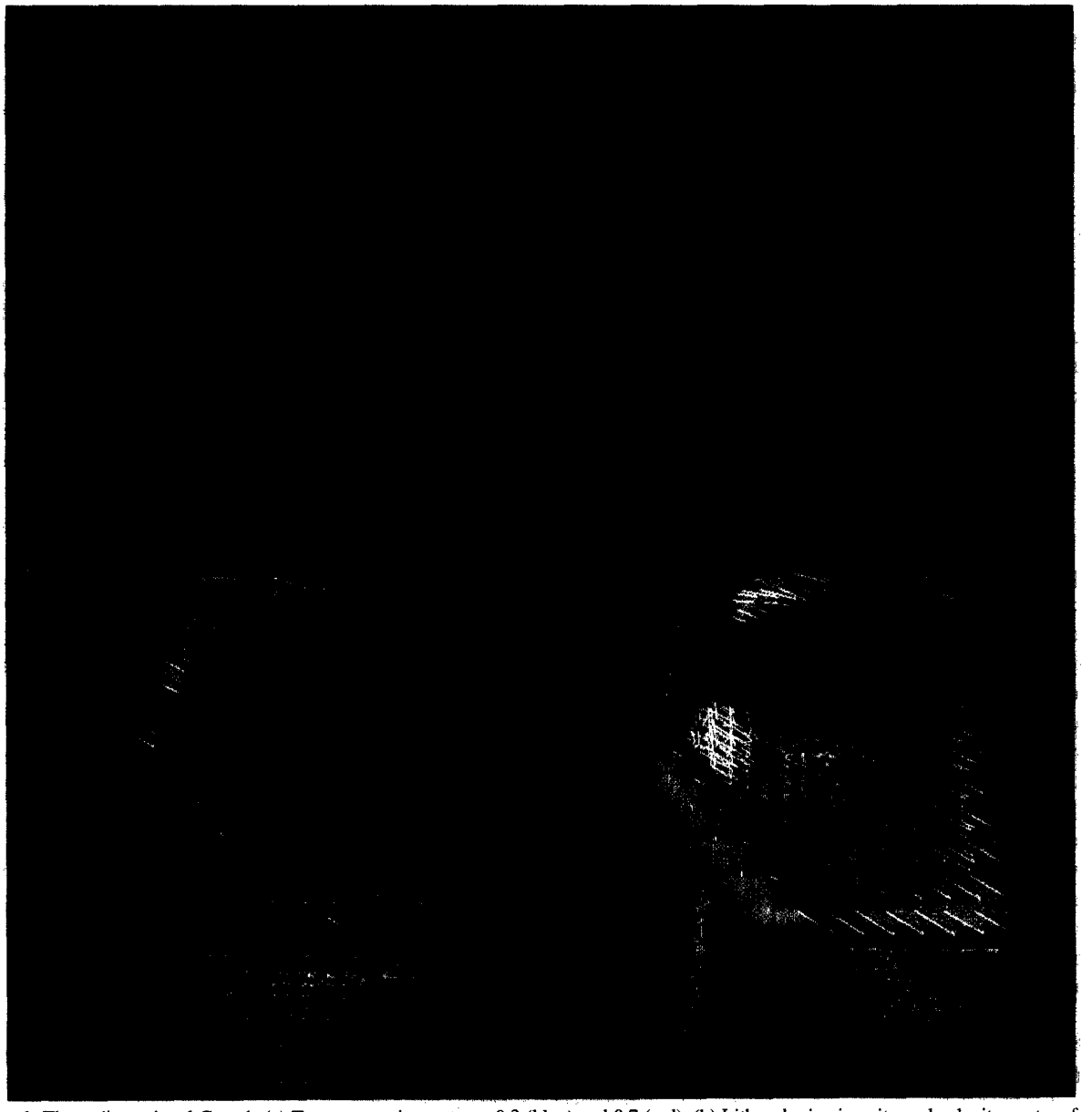

Fig. 3. Three-dimensional Case 1. (a) Temperature isocontours 0.3 (blue) and 0.7 (red). (b) Lithospheric viscosity and velocity vectors for SRW rheology. Viscosity ranges from 0.1 (violet) to 10^4 (orange), and the maximum velocity value is 670. (c) Isocontours of horizontal divergence/convergence (±50, light and dark purple) and vertical vorticity (±50, green and blue) for SRW rheology.

Fig. 4. Three-dimensional Case 2. (a) Residual temperature isocontours 0.15 (red) and −0.15 (blue). (b) Lithospheric viscosity and velocity vectors for SRW rheology. Maximum velocity in the domain is 780. (c) Isocontours of horizontal divergence (±50, green and blue) and vertical vorticity (±25, yellow and mauve) and for SRW rheology. (d) As (b) for visco-plastic rheology. (e) As (c) for visco-plastic rheology. Horizontal divergence (±40, green and blue) and vertical vorticity (±10, yellow and mauve).

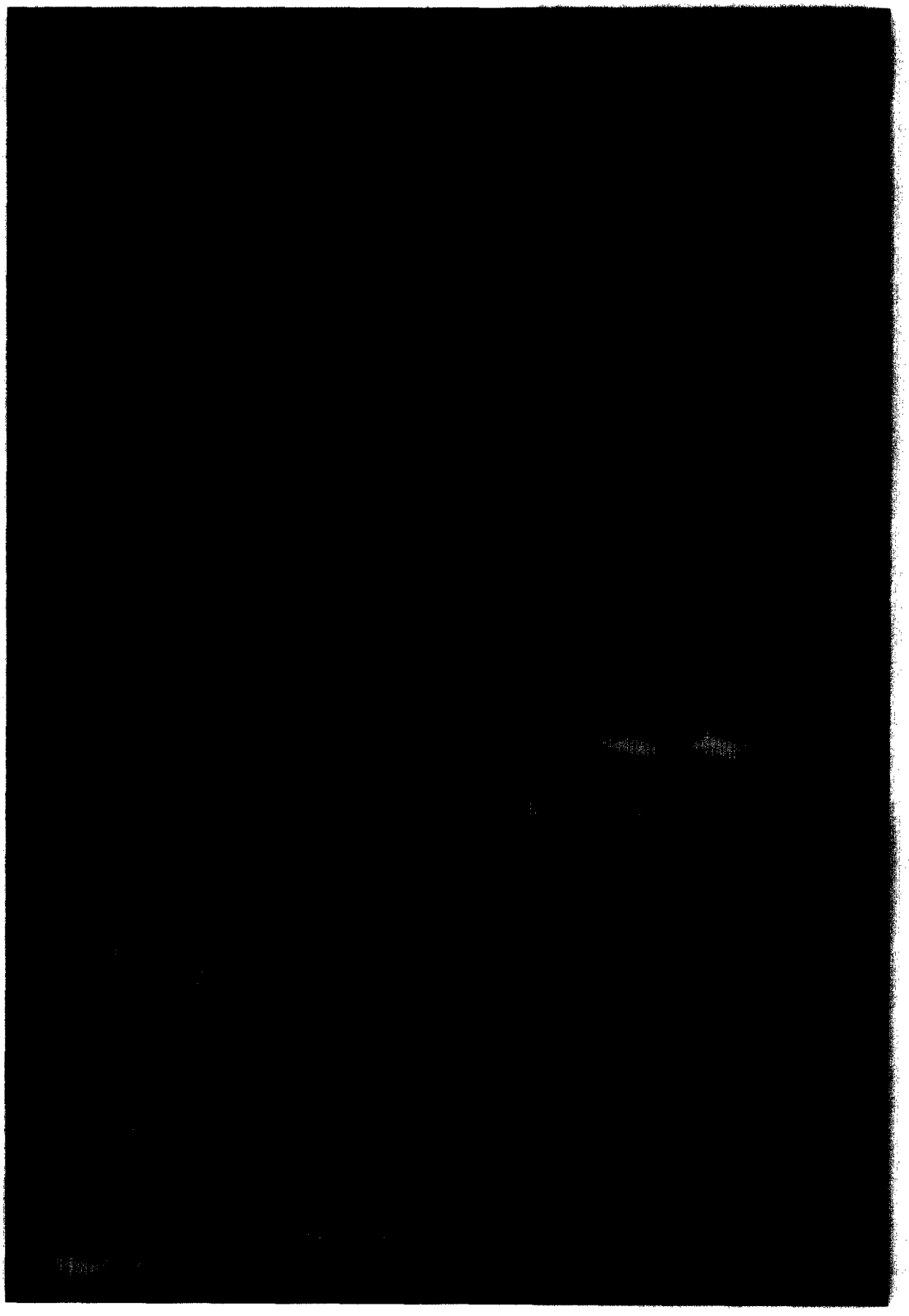

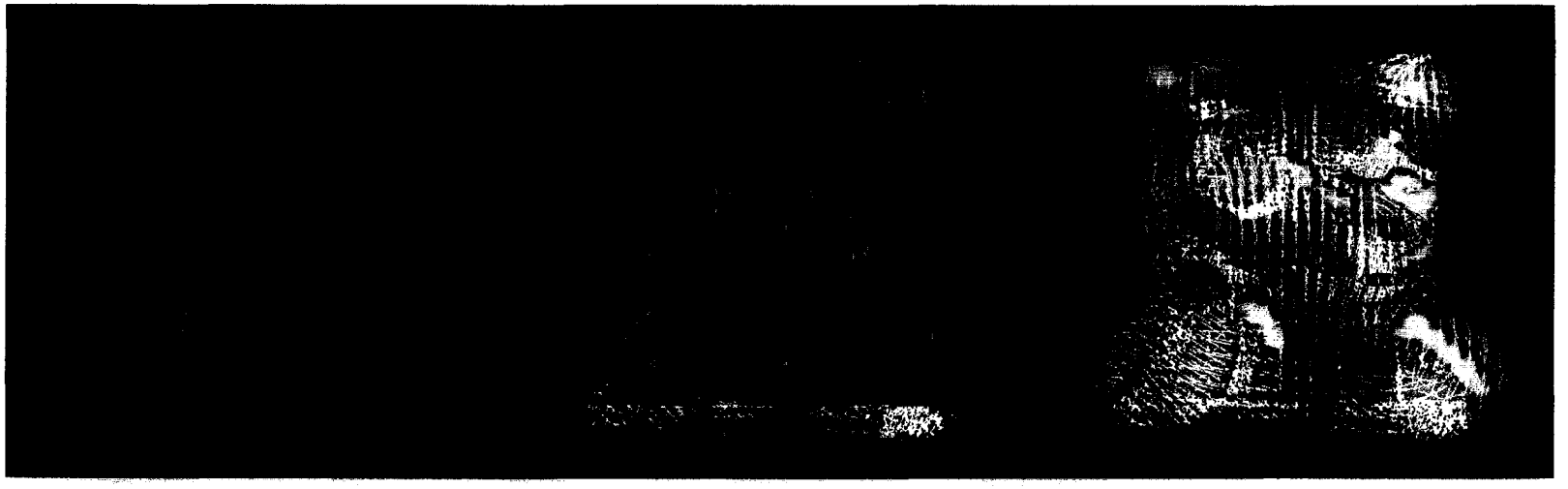

Fig. 5. Three-dimensional Case 3. (a) Residual temperature isocontour −0.15. (b) Lithospheric viscosity and velocity vectors (domain maximum velocity is 302). (c) Horizontal divergence (±35, green and blue) and vertical vorticity (±20, yellow and mauve).

Fig. 6. Three-dimensional Case 4. As Fig. 5 except (a) residual temperature isocontours 0.15 (red) and −0.15 (green), domain maximum velocity is 2030. (c) Horizontal divergence (±200) and vertical vorticity (±150).

is more complex, with typically four microplates. The location of these passive spreading centers can be understood by examining the stress distribution for an isoviscous case: a secondary stress maximum ('halo') appears at a characteristic distance from the down-welling.

While the overall pattern does not appear particularly Earth-like, it is very encouraging that passive spreading centers have formed, since mid-ocean ridge spreading centers on Earth are believed to be passive, i.e. with no strong active up-welling beneath them [43].

5.4. Compressible formulation, basal heating (Fig. 6)

Here, the temperature field appears the most 'Earth-like' of the cases, with long linear down-wellings and a broad 'megaplume', similar to those observed in global seismic tomographic models [44–46]. Again, the pattern is characterized by up-/down-welling WZs with width comparable to the convective features and predominantly convergent/divergent motion, interconnected by narrow WZs with high vorticity. Several plates have appreciable rotation; probably a consequence of the geometrical constraints.

5.5. Multiple solutions?

As with the 1- and 2-D cases, the possibility of multiple solutions arises from the fact that each stress has two strain-rate values. For these 3-D results, however, the presence of thermal driving sources breaks the symmetry of the system, and appears to lead to a robust solution, where WZs form along up- and down-wellings and along lines of initial stress maxima between them. Indeed, the final solution can be fairly well predicted by looking at the lithospheric stress distribution for an isoviscous solution.

6. Discussion and conclusions

A strain-rate-weakening (SRW) rheology, which may be a generic, 'steady-state' representation of strain-weakening mechanisms observed in nature, is very effective in producing plate-like behavior in the two-dimensional lithosphere of a 3-D mantle convection, whereas a simple visco-plastic rheology does not produce good plate-like behavior. (Although an *elasto*-plastic rheology does produce shear localization, e.g. [47]). The system forms high viscosity plates separated by low-viscosity 'weak zones' (WZ), with a sharp, well-defined transition between the plates and WZs. WZs form above up- and down-wellings, and also in lines connecting the up- and down-wellings. The up-/down-welling WZs have a width comparable to the width of the up- or down-welling, and are associated with predominant convergence or divergence. The interconnecting WZs are narrow, localizing to a size which is related to the viscosity of the underlying medium, and exhibit strong vertical vorticity, implying strike-slip motion. However, most WZs display a mixture of strike-slip and convergent/divergent behavior. In 100% internally heated cases, 'microplates' next to the down-wellings are formed in an otherwise fairly stagnant lid, involving the formation of passive spreading centers.

The ability to form *weak* strike-slip margins is probably fundamental in producing plates, since there are no buoyancy forces which can directly drive and localize strike-slip motion. If transform boundaries were strong, as they would be with a purely visco-plastic rheology, mantle convection would not arrange itself to drive them, but would likely form a system of rolls, as far as possible.

Although these results are very encouraging, the 'plates' are not completely Earth-like. This is not surprising considering the simplifications involved in the model: lack of elasticity, almost two-dimensional lithosphere, very simplified rheology, and fairly coarse resolution (relative to the size of 'real' faults). How may these shortcomings may be overcome in the future?

6.1. Size

The plates are too small, compared to plates on Earth. This may improve when the system is allowed to evolve in time. Some plates will grow, while others will shrink and eventually disappear. Meanwhile, it will be difficult for new plate boundaries to form because existing plate boundaries prevent sufficient stress from building up. This may result in a pattern with fewer, larger plates.

6.2. Passive spreading centers

The Earth's mantle, to first order, resembles an internally heated system, but the internally heated cases look un-Earth-like. What is required is passive spreading centers far from down-wellings and separating them, rather than restricted to the immediate vicinity of down-wellings. If the lithosphere is generated by temperature-dependent viscosity, rather than being of constant thickness, passive spreading centers are naturally weak due to the thinness of the lithosphere, which facilitates their existence. Indeed, an SRW rheology is not necessary to generate and maintain them: two-dimensional models indicate that a simple yield stress is all that is necessary (V.S. Solomatov, personal communication; author, unpublished results).

6.3. Plate margins

Realistic plate margins are not formed, in particular, single-sided subduction and pure transform boundaries (with no convergence or divergence). The inclusion of elasticity may give a more 'fault-like' character to plate margins. High resolution may, if accompanied by greater localization, lead to WZs which allow shear, but make convergence or divergence difficult (since they would involve 'squishing' material through the narrow channel out of the shear zone). However, localization is ultimately limited by the parameterization, not by resolution. Clearly, a more realistic physical description is necessary. For example, at subduction zones, two weakening mechanisms may be operating: one to make the slab weak enough to bend around the corner, and another to generate the shear zone between the slab and overlying plate.

6.4. Memory

The simple system modeled here has a weak type of memory due to the nature of the rheology (2 strain-rate values for each stress), which leads, in principle, to multiple solutions for the plates. The solution obtained is thus dependent on the initial conditions of the numerical iteration process, which is the previous timestep's solution in a time-dependent calculation. This needs to be investigated in detail.

The next logical step in terms of physical reality and parameterization is a description where the time accumulation of strain-weakening 'damage' (e.g. grain-size reduction, microcracks, voids, volatile infiltration) is explicitly tracked, and also allowed to heal with time. Such a description has memory built-in. The present SRW-rheology corresponds to a generalized 'steady-state' version of the damage production + healing process, as discussed earlier.

6.5. Inhomogeneous lithosphere

A result of 'memory' is that the lithosphere is not homogeneous, but is riddled with zones of weakness generated during its history. Another obvious source of differences in lithospheric strength is the continent–ocean distinction. It is clear that issues of lithospheric heterogeneity and memory are important and must be included in future plate generation studies.

6.6. Future directions

The results presented here show, for the first time, that self-consistent plate generation is a realizable goal in global mantle convection models. However, the present model is far from a realistic Earth and many improvements must be made.

In order for the model presented here to be fully self-consistent: (1) the system should be evolved in time, so that the thermal field and plates adjust to one another; (2) the lithosphere should be generated through temperature-dependent rheology, rather than being imposed as a constant-thickness layer; (3) it will be important to use a physically realistic material description which tracks the production and healing of 'damage' instead of using an idealized 'steady-state' rheology; and finally, (4) elasticity should be included due to its importance in the upper lithosphere and crust.

Acknowledgements

Useful discussions were had with Shun-Ichiro Karato and David Bercovici. Thoughtful reviews by S.-I. Karato and 'anonymous' improved the

manuscript. Supported by NASA and the National Science Foundation. 3-D calculations were performed on the Cray T3E at San Diego Supercomputer Center, and the Cray T3E at Nasa Goddard Space Flight Center. *[RV]*

References

[1] J.T. Ratcliff, P.J. Tackley, G. Schubert, A. Zebib, Transitions in thermal convection with strongly variable viscosity, Phys. Earth Planet. Inter. 102 (1997) 201–212.

[2] V.S. Solomatov, Scaling of temperature-dependent and stress-dependent viscosity convection, Phys. Fluids 7 (1995) 266–274.

[3] H.P. Bunge, M.A. Richards, The origin of large-scale structure in mantle convection – effects of plate motions and viscosity stratification, Geophys. Res. Lett. 23 (1996) 2987–2990.

[4] S.J. Zhong, M. Gurnis, Interaction of weak faults and non-Newtonian rheology produces plate-tectonics in a 3d model of mantle flow, Nature 383 (1996) 245–247.

[5] S.D. King, J. Ita, Effect of slab rheology on mass-transport across a phase-transition boundary, J. Geophys. Res. 100 (1995) 20211–20222.

[6] G. Ranalli, Rheology of the Earth, Chapman and Hall, London, 1995, 413 pp.

[7] L.E. Gilbert, C.H. Scholz, J. Beavan, Strain localization along the San Andreas fault – consequences for loading mechanisms, J. Geophys. Res. 99 (1994) 23975–23984.

[8] K.P. Furlong, S.M. Atkinson, Seismicity and thermal structure along the northern San-Andreas fault system, California, USA, Tectonophysics 217 (1993) 23–30.

[9] D. Jin, S.-I. Karato, M. Obata, Mechanisms of shear localization in the continental lithosphere: inference from the deformation microstructures of peridotites from the Ivrea zones, northwest Italy, J. Struct. Geol., in press.

[10] U. Christensen, Convection with pressure-dependent and temperature-dependent non-Newtonian rheology, Geophys. J. R. Astron. Soc. 77 (1994) 343–384.

[11] L. Cserepes, Numerical studies of non-Newtonian mantle convection, Phys. Earth Planet. Inter. 30 (1982) 49–61.

[12] S.A. Weinstein, P.L. Olson, Thermal convection with non-Newtonian plates, Geophys. J. Int. 111 (1992) 515–530.

[13] S.A. Weinstein, Thermal convection in a cylindrical annulus with a non-Newtonian outer surface, Pure Appl. Geophys. 146 (1996) 551–572.

[14] C. Lithgow-Bertelloni, M.A. Richards, Y. Ricard, R.J. O'Connell, D.C. Engebretson, Toroidal–poloidal partitioning of plate motions since 120 Ma, Geophys. Res. Lett. 20 (1993) 375–378.

[15] C.W. Gable, R.J. O'Connell, B.J. Travis, Convection in 3 dimensions with surface plates – generation of toroidal flow, J. Geophys. Res. 96 (1991) 8391–8405.

[16] N.M. Ribe, The dynamics of thin shells with variable viscosity and the origin of toroidal flow in the mantle, Geophys. J. Int. 110 (1992) 537–552.

[17] U. Christensen, H. Harder, 3-D convection with variable viscosity, Geophys. J. Int. 104 (1991) 213–226.

[18] S.A. Weinstein, The effect of convection planform on the toroidal–poloidal energy ratio, Geophys. J. Int., submitted.

[19] D. Bercovici, A simple model of plate generation from mantle flow, Geophys. J. Int. 114 (1993) 635–650.

[20] R.L.M. Vissers, M.R. Drury, E.H.H. Strating, C.J. Spiers, D. Vanderwal, Mantle shear zones and their effect on lithosphere strength during continental breakup, Tectonophysics 249 (1995) 155–171.

[21] M.R. Drury, R.L.M. Vissers, D. Vanderwal, E.H.H. Strating, Shear localization in upper mantle peridotites, Pure Appl. Geophys. 137 (1991) 439–460.

[22] K. Sorensen, Growth and dynamics of the Nordre-Stromfjord shear zone, J. Geophys. Res. 88 (1983) 3419–3437.

[23] G.E. Jaroslow, G. Hirth, H.J.B. Dick, Abyssal peridotite mylonites – implications for grain-size sensitive flow and strain localization in the oceanic lithosphere, Tectonophysics 256 (1996) 17–37.

[24] S.I. Karato, M.S. Paterson, J.D. Fitzgerald, Rheology of synthetic olivine aggregates – influence of grain-size and water, J. Geophys. Res. 91 (1986) 8151–8176.

[25] S.-I. Karato, M. Toriumi, T. Fujii, Dynamic recrystallization of olivine single crystals during high-temperature creep, J. Geophys. Res. 7 (1980) 649–652.

[26] M. Kameyama, D.A. Yuen, H. Fujimoto, The interaction of viscous heating with grain-size dependent rheology in the formation of localized slip zones, Geophys. Res. Lett. 24 (1997) 2523–2526.

[27] D. Bercovici, Generation of plate tectonics from lithosphere–mantle flow and void-volatile self-lubrication, Earth Planet. Sci. Lett. 154 (1998) 139–151.

[28] K. Regenauer-Lieb, Dilatant plasticity applied to Alpine collisions: ductile void growth in the intraplate area beneath the Eifel volcanic field, J. Geodyn., in press.

[29] D.A. Yuen, L. Fleitout, G. Schubert, C. Froidevaux, Shear deformation zones along major transform faults and subducting slabs, Geophys. J. R. Astron. Soc. 54 (1978) 93–119.

[30] L. Fleitout, C. Froidevaux, Thermal and mechanical evolution of shear zones, J. Struct. Geol. 2 (1980) 159–164.

[31] M. Obata, S. Karato, Ultramafic pseudotachylite from the Balmuccia peridotite, Ivrea Verbano zone, Northern Italy, Tectonophysics 242 (1995) 313–328.

[32] V. Lyakhovsky, Y. Podladchikov, A. Poliakov, A rheological model of a fractured solid, Tectonophysics 226 (1993) 187–198.

[33] K.C. Valanis, A theory of damage in brittle materials, Eng. Fract. Mech. 36 (1990) 403–416.

[34] N.R. Hansen, H.L. Schreyer, A thermodynamically consistent framework for theories of elastoplasticity coupled with damage, Int. J. Sol. Struct. 31 (1994) 359–389.

[35] D. Bercovici, A source–sink model of the generation of plate-tectonics from non-Newtonian mantle flow, J. Geophys. Res. 100 (1995) 2013–2030.

[36] D. Bercovici, Plate generation in a simple model of lithosphere-mantle flow with dynamic self-lubrication, Earth Planet. Sci. Lett. 144 (1996) 41–51.
[37] P.J. Tackley, Effects of strongly temperature-dependent viscosity on time-dependent, Three-dimensional models of mantle convection, Geophys. Res. Lett. 20 (1993) 2187–2190.
[38] P.J. Tackley, Effects of strongly variable viscosity on three-dimensional compressible convection in planetary mantles, J. Geophys. Res. 101 (1996) 3311–3332.
[39] S. Balachandar, D.A. Yuen, D.M. Reuteler, High Rayleigh number convection at infinite Prandtl number with weakly temperature-dependent viscosity, Geophys. Astrophys. Fluid Dyn. 83 (1996) 79–117.
[40] S. Balachandar, D.A. Yuen, D.M. Reuteler, Localization of toroidal motion and shear heating in 3-D high Rayleigh number convection with temperature-dependent viscosity, Geophys. Res. Lett. 22 (1995) 477–480.
[41] P.J. Tackley, On the ability of phase transitions and viscosity layering to induce long-wavelength heterogeneity in the mantle, Geophys. Res. Lett. 23 (1996) 1985–1988.
[42] B. Travis, S. Weinstein, P. Olson, Three-dimensional convection planforms with internal heat generation, Geophys. Res. Lett. 17 (1990) 243–246.
[43] G.F. Davies, Ocean bathymetry and mantle convection. 1. Large-scale flow and hotspots, J. Geophys. Res. 93 (1988) 10467–10480.
[44] Y. Fukao, Seismic tomogram of the Earths mantle – geodynamic implications, Science 258 (1992) 625–630.
[45] W.J. Su, R.L. Woodward, A.M. Dziewonski, Degree-12 model of shear velocity heterogeneity in the mantle, J. Geophys. Res. 99 (1994) 6945–6980.
[46] G. Masters, S. Johnson, G. Laske, H. Bolton, A shear-velocity model of the mantle, Phil. Trans. R. Soc. Lond. A354 (1996) 1385–1410.
[47] A.N.B. Poliakov, H.J. Herrmann, Self-organized criticality of plastic shear bands in rocks, Geophys. Res. Lett. 21 (1994) 2143–2146.